

Figure 3. View of the structure of newberyite, $\text{MgHPO}_4 \cdot 3\text{H}_2\text{O}$.⁸ In the structure proposed for $\text{VO}(\text{C}_6\text{H}_5\text{PO}_3) \cdot 2\text{H}_2\text{O}$, V replaces Mg in newberyite, a phenyl group replaces the hydroxyl group on phosphorus, and the stippled water molecule is replaced by a vanadyl oxygen atom.

examples condensation occurs between layers rather than within a single layer. The formation of chains within a layer results in an available area of 68 \AA^2 to accommodate two pendant phenyl groups on each side of the layer. Each phenyl group has van der Waals dimensions of approximately $3.6 \times 6.3 = 23 \text{ \AA}^2$, consequently phenyl groups from adjacent layers cannot interpenetrate completely but instead form a bilayer arrangement as shown in Figure 1. In contrast, the presence of an extra water molecule coordinated to vanadium in the dihydrate structure increases the layer area to 98 \AA^2 , sufficient to allow a structure with interpenetrating phenyl groups.

The magnetic susceptibilities of both compounds were measured over the temperature range 4–300 K. The reciprocal susceptibility data for the dihydrate were linear over the whole temperature range, while corresponding data for the monohydrate exhibit an increase in inverse susceptibility below $\sim 15 \text{ K}$, reflecting antiferromagnetic coupling along the $-\text{V}=\text{O}-\text{V}-$ chains. At higher temperatures both compounds have susceptibilities close to the value calculated for V^{4+} ions with $S = 1/2$ and $g = 2$. The detailed form of $\chi(T)$ for the monohydrate has not yet been fully analyzed but will be described in detail in a future publication.¹⁰

The similarity between the two structures suggests that they might be interconvertible. Dehydration of the dihydrate below $210 \text{ }^\circ\text{C}$ does not lead to structural rearrangement, and intercalation of alcohols or water into the resulting monohydrate remains a reversible process. Attempts to break the $-\text{V}=\text{O}-\text{V}-$ chains in the hydrothermally synthesized monohydrate have been partially successful. For example, a very slow reaction with hexanol is observed at $150 \text{ }^\circ\text{C}$ which may indicate reformation of the dihydrate type layers.¹¹ In principle, the two struc-

tures can be interconverted topotactically without breaking any bonds other than those between the trans water molecule and the vanadium atom. In practice, the two phases are difficult to interconvert below the temperature at which the cis water molecule is lost because of the extensive reorganization of the structure required by the repacking of the organic groups. The formation of the two phases under the different synthetic conditions can be understood. The dihydrate structure is obtained in the presence of ethanol which is incorporated during the reaction coordinated trans to the vanadyl oxygen. The presence of this coordinating molecule stabilizes formation of the more open dihydrate layer structure. In a subsequent step this ethanol molecule is replaced by water to form the dihydrate. The monohydrate is formed at temperatures above the decomposition temperature of the dihydrate.

The layered compound $\text{VO}(\text{C}_6\text{H}_5\text{PO}_3) \cdot \text{H}_2\text{O}$ has been prepared and characterized by single-crystal X-ray diffraction. The structure is consistent with and supports the previously proposed structural model for the dihydrate. The two structures are similar in the V–P–O connectivity but are substantially different in the organization of the organic interlayers. Comparison of the two compounds illustrates the complex interplay that occurs between the inorganic layer connectivity and the interlayer organic packing in determining the overall structure of systems with alternating inorganic and organic layers.

Acknowledgment. We thank D. P. Goshorn and J. P. Stokes for the magnetic susceptibility measurements.

Supplementary Material Available: Tables of atomic positional and isotropic equivalent thermal parameters, anisotropic thermal parameters, least-squares planes, and bond distances and angles and a diagram showing thermal ellipsoids and atom labels (6 pages); observed and calculated structure factors (6 pages). Ordering information is given on any current masthead page.

Morphological and Compositional Characterization of Copper–Cobalt Spinel Made by Mechanochemical Reactions

Ranko P. Bonchev

*Institute of General and Inorganic Chemistry
Acad. G. Bonchev Str., bl. 11
Sofia 1040, Bulgaria*

Tsvetanka Zheleva and Slavi C. Sevov*

*Institute of Applied Mineralogy
92 Rakovska Str., Sofia 1000, Bulgaria*

Received December 5, 1989

Copper–cobalt spinels with general formula $\text{Cu}_x\text{Co}_{3-x}\text{O}_4$ ($x < 1.0$) are well-known for their high catalytic activity toward the oxidation of CO to CO_2 . Furthermore when $x > 0.6$, they remain active even in the presence of a catalytic poison such as SO_2 .¹⁻⁴

(9) Ladwig, G. Z. *Anorg. Allg. Chem.* **1965**, *338*, 266–278. Johnson, J. W.; Jacobson, A. J.; Brody, J. F.; Rich, S. M. *Inorg. Chem.* **1982**, *21*, 3820–3825. Johnson, J. W.; Johnston, D. C.; Jacobson, A. J.; Brody, J. F. *J. Am. Chem. Soc.* **1984**, *106*, 8123–8128. Bordes, E.; Courtine, P.; Johnson, J. W. *J. Solid State Chem.* **1984**, *55*, 270–279.

(10) Huan, G.; Goshorn, D. P.; Jacobson, A. J.; et al., to be submitted.

(11) Treatment of powdered $\text{VO}(\text{C}_6\text{H}_5\text{PO}_3) \cdot \text{H}_2\text{O}$ with hexanol under refluxing conditions results in partial (17%) intercalation of the alcohol as indicated by powder X-ray diffraction (a second 00l line, observed at 15.2 \AA) and thermogravimetric analysis. Attempts to remove the intercalate with water at $70 \text{ }^\circ\text{C}$ for 3 days were unsuccessful, suggesting a strong interaction between the alcohol and the layered material.

*To whom the correspondence should be addressed at: 345 Spedding, Ames Laboratory, Iowa State University, Ames, IA 50011.

(1) Mehandjiev, D.; Piperov, B. *Heterog. Katal., Varna* **1975**, 405.
(2) Angelov, S.; Zhecheva, E.; Petrov, K.; Mehandjiev, D. *Mater. Res. Bull.* **1982**, *17*, 235.
(3) Zhecheva, E.; Angelov, S.; Mehandjiev, D. *Thermochim. Acta* **1983**, *67*, 91.
(4) Angelov, S.; Mehandjiev, D.; Piperov, B.; Zarkov, V.; Terlecki-Baricevic, A.; Jovanovic, D.; Jovanovic, Z. *Appl. Catal.* **1985**, *16*, 431.

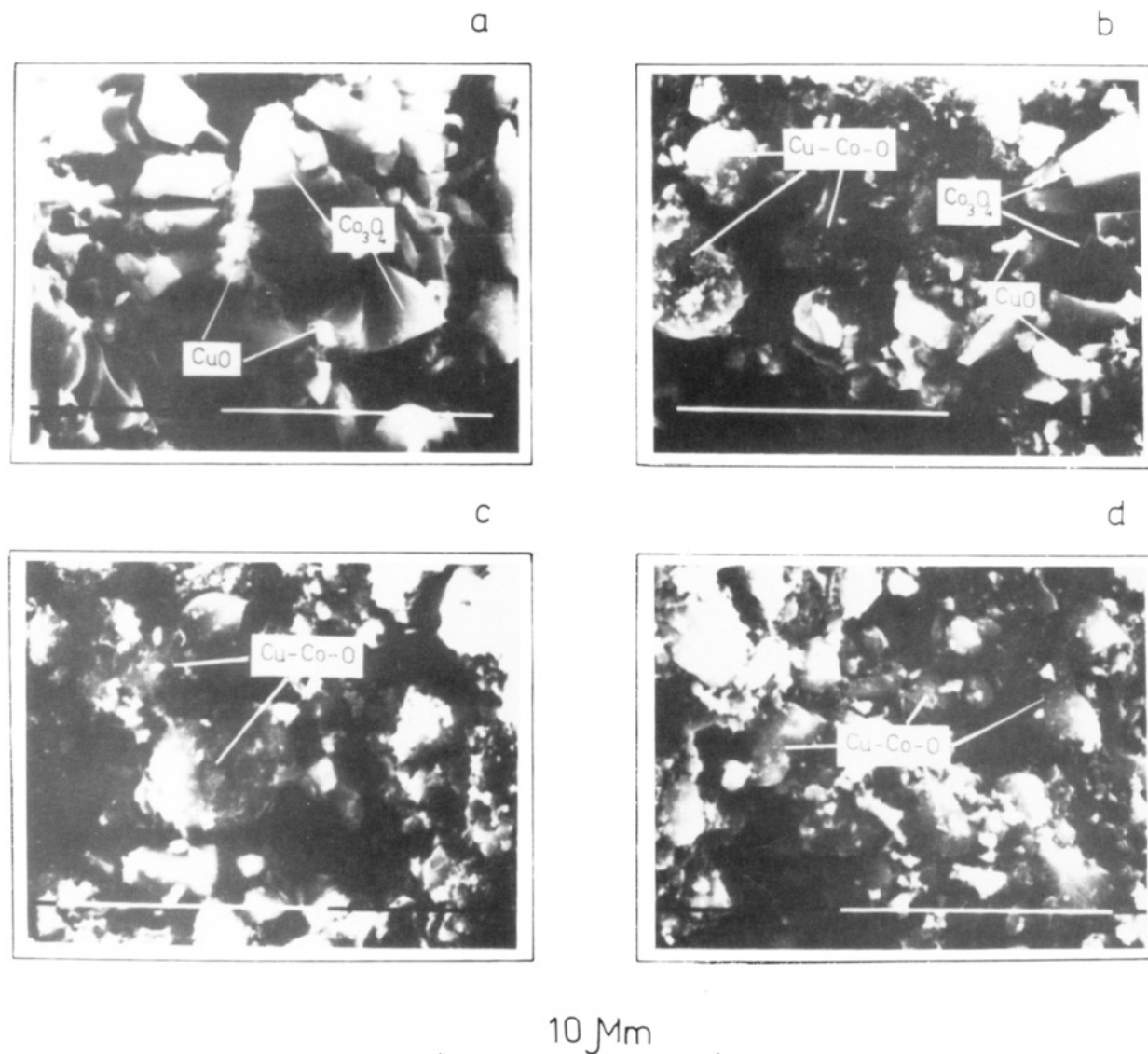


Figure 1. SEM pictures taken from a mixture $\text{CuO}:\text{Co}_3\text{O}_4 = 1:5$ after: (a) 0, (b) 5, (c) 8, and (d) 15 h of grinding.

We have shown that the product of a mechanochemical reaction between CuO and Co_3O_4 shows the same catalytic properties as the spinel made by other more conventional methods.⁵⁻⁷ It has been found that the two oxides are involved in a solid-state reaction during the treatment, and after a long enough time the CuO (the molar ratio of CuO to Co_3O_4 was 0.2) is practically consumed.⁸⁻¹³ The X-ray powder diffraction patterns of the final product showed that besides the Co_3O_4 another spinel with slightly larger lattice parameter was formed.^{5,7,14}

We present here the chemical composition, the phase composition, and the morphology of this product.

In a typical reaction, CuO (Chemapol, 99.99%) and Co_3O_4 made by thermal decomposition of $\text{Co}(\text{NO}_3)_2 \cdot 6\text{H}_2\text{O}$

(Merck, 99.99%) at 230 °C were mixed in molar ratio 1:5. The mixture was homogenized as an alcohol suspension, dried at 70 °C, and ground in a frictional grinder (Fritsch) with agate set for 15 h at room temperature. The electron microscopy investigations were accomplished on Philips 420 TEM and Philips 515 SEM equipped with EDAX systems for elemental microanalyses. The high-resolution transmission-electron micrographs were processed on a Kontron image analyser.

Pictures on a SEM were taken from the mixture before and after 5, 8, and 15 h of treatment in the frictional grinder (Figure 1). It can be seen that the particles' morphology depends upon the time of grinding. The big sharp-edged chunks of Co_3O_4 and the small pieces of CuO start disappearing, and at the same time rather rounded particles containing simultaneously Cu and Co form. Selected area electron diffraction (SAED) from the latter showed that they were of a spinel structure. The atomic ratio of Cu to Co determined by microprobe elemental analyses on these particles was in the range 0.1–0.5.

The electron polycrystalline diffraction from the samples showed that the CuO is practically consumed after 15 h of grinding. While the lines of CuO can be seen in the diffraction patterns of samples treated less than 8 h, those lines do not exist after 15 h of grinding. The only structure seen in the latter is of a spinel type. These observations are in agreement with X-ray diffraction findings.

(5) Angelov, S.; Bonchev, R. *App. Catal.* **1986**, *24*, 219.

(6) Angelov, S.; Bonchev, R. *Proc. VIth Int. Symp. Heterog. Catal.*, Sofia **1987**.

(7) Angelov, S.; Bonchev, R. *Dokl. Bolg. Akad. Nauk.* **1987**, *40*, 63.

(8) Liahov, H. Z.; Boldirev, V. V. *Izv. Sib. Acad. Nauk. USSR, Ser. Chim.* **1982**, *5*, 3.

(9) Tretiakov, Y. D. *Tverdophasnie Reakzii*; Chimia: Moscow, 1978.

(10) Avvakumov, E. G. *Mehanicheskie metodi aktivatzii chimicheskikh procesov*; Nauka: Novosibirsk, 1986.

(11) Angelov, S.; Zhecheva, E.; Mehandjiev, D. *Comm. Dept. Chem. Bulg. Acad. Sci.* **1980**, *13*, 369.

(12) Angelov, S.; Tyuliev, G.; Marinova, Ts. *Appl. Surf. Sci.* **1987**, *27*, 387.

(13) Tyuliev, G.; Angelov, S. *Appl. Surf. Sci.* **1988**, *32*, 381.

(14) Bonchev, R.; Angelov, S., to be submitted for publication.

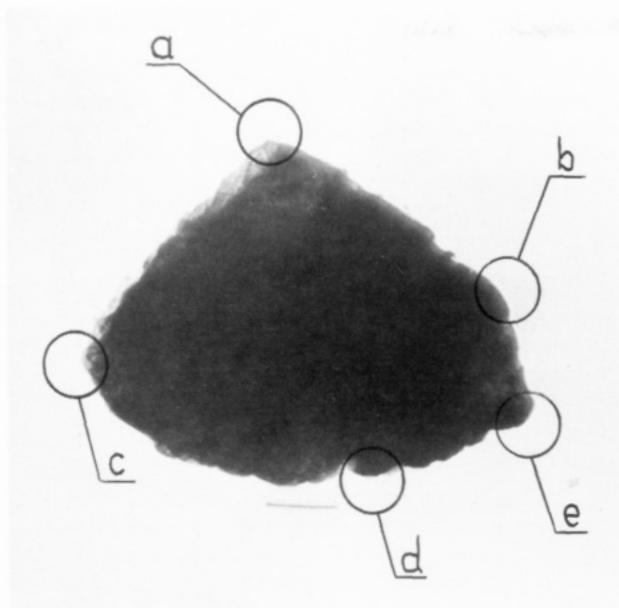


Figure 2. TEM picture of a typical particle from the mixture $\text{CuO}:\text{Co}_3\text{O}_4 = 1:5$ ground for 15 h. The atomic ratio of Cu to Co is (a) 0.44, (b) 0.46, (c) 0.44, (d) 0.41, and (e) 0.44.

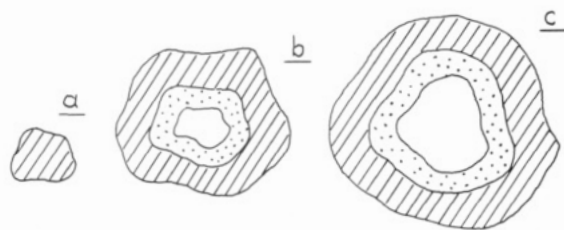


Figure 3. Model for the compositional cross section of particles with different sizes (a-c) found in the product of 15 h of ground mixture $\text{CuO}:\text{Co}_3\text{O}_4$ (1:5). The average atomic Cu concentration is 30% in the dashed region, 10% in the dotted region, and 0% in the blank region.

The next question to be answered was whether the copper was distributed homogeneously or not within the particles of the product. It was noticed that smaller particles showed higher Cu concentration than the larger ones. This led to the idea that the Cu is only in a surface layer with approximately the same thickness in all particles. To check this, the structure and the composition of a layer approximately 50 nm thick were carefully determined. SAED showed that the layer possessed a spinel structure, and no other phases were seen. The atomic ratio of Cu and Co was measured at different edges of a particle (Figure 2). It remained essentially the same for all points and fell in the range 0.41–0.46. Such a ratio corresponds to a spinel with an approximate composition $\text{Cu}_{0.9}\text{Co}_{2.1}\text{O}_4$. More analyses were done at the edges of many other particles, and they showed the same composition. From the initial quantity of CuO and the calculated for the 50-nm-thick layer of $\text{Cu}_{0.9}\text{Co}_{2.1}\text{O}_4$ there had to be some extra Cu in the product. A profile fitting of an X-ray diffraction spectrum of the same sample has shown that x in $\text{Cu}_x\text{Co}_{3-x}\text{O}_4$ varies from 0 to 0.9 rather than being constant and equal to 0.9.¹⁵ This result suggests that the copper penetrates even deeper than 50 nm into the particles of Co_3O_4 .

Summing all the information, a model for the composition of the final product can be proposed. The very small

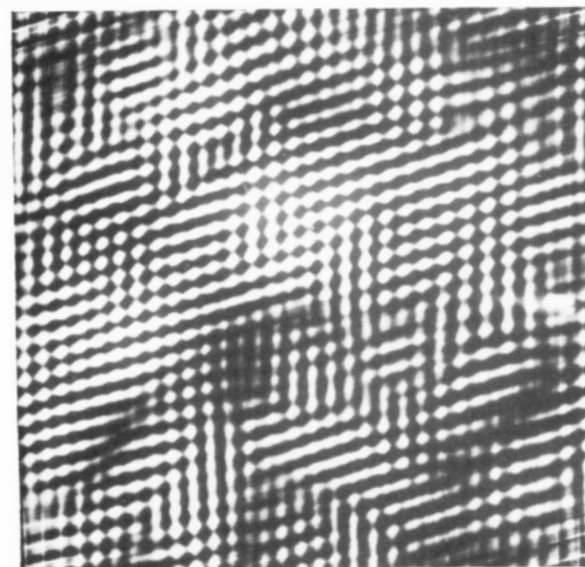
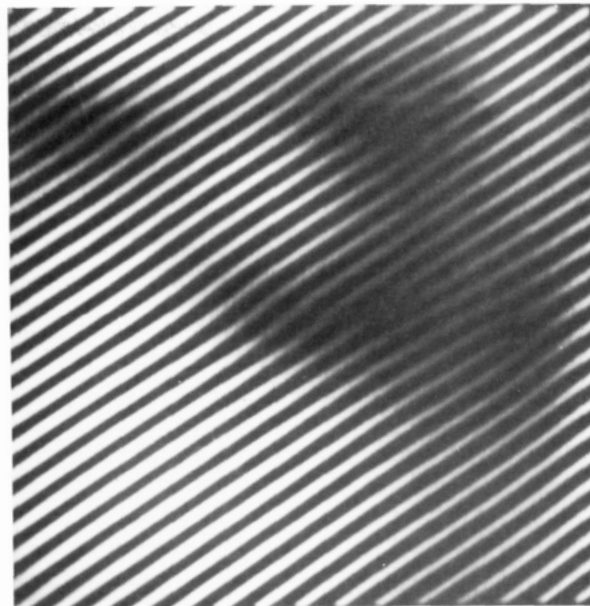


Figure 4. HREM micrographs showing (a) one-dimensional defects in (111) type planes and (b) two-dimensional defects in the (110) reciprocal plane.

particles have high and almost uniform copper concentration throughout the particle (Figure 3a). In the bigger particles x in $\text{Cu}_x\text{Co}_{3-x}\text{O}_4$ varies from 0.9 on the surface to virtually zero deeper in the particle (Figure 3b,c). This explains the differences in the total copper concentration for the small and the large particles. The Cu concentration has a smoother profile than represented by Figure 3.

High-resolution micrographs taken on a TEM from the surface layer of the particles in the product show high concentrations of one- and two-dimensional defects (Figure 4). This gives rise to high surface energy, which itself can account for the chemical properties of the mechanochemically made copper-cobalt spinel.

In conclusion, by a mechanochemical reaction between CuO and Co_3O_4 a catalytically active surface layer of $\text{Cu}_{0.9}\text{Co}_{2.1}\text{O}_4$ is formed on particles of Co_3O_4 . Since the catalytic processes are surface processes, these particles act in the same way as bulk $\text{Cu}_{0.9}\text{Co}_{2.1}\text{O}_4$ prepared by other methods.

Registry No. CuO, 1317-38-0; Co_3O_4 , 1308-06-1; $\text{Co}_{2.1}\text{Cu}_{0.9}\text{O}_4$, 110619-40-4.

(15) Kovacheva, D.; Bonchev, R.; Petrov, K., to be submitted for publication.